Available online at www.sciencedirect.com
ScienceDirect
Trans. Nonferrous Met. Soc. China 32(2022) 3469−3477
Transactions of Nonferrous Metals Society of China
www.tnmsc.cn

Preparation of low-oxygen Ti powder from TiO_2 through combining self-propagating high temperature synthesis and electrodeoxidation

Xin-yu ZHOU[1,2], Zhi-he DOU[1,2], Ting-an ZHANG[1,2], Ji-sen YAN[2], Jian-peng YAN[2]

1. Key Laboratory of Ecological Metallurgy of Multi-metal Intergrown Ores of Ministry of Education, Northeastern University, Shenyang110819, China;
2. School of Metallurgy, Northeastern University, Shenyang 110819, China

Received 30 August 2021; accepted 25 February 2022

Abstract: An effective method was reported to prepare low-oxygen Ti powder, which included two experimental steps: the fast conversion of TiO_2 to $TiO_{x<1}$ powder by self-propagating high-temperature synthesis (SHS) process and the generation of low-oxygen Ti powder by electrodeoxidizing $TiO_{x<1}$ powder at the cathode in molten $CaCl_2$. The key intermediate steps were analyzed by XRD, SEM and electrochemical testing techniques. The results demonstrated that $TiO_{x<1}$ powder ($TiO_{0.325}$ and $TiO_{0.97}$) was generated after acid leaching MgO in SHS products with TiO_2/Mg molar ratio of 1:2, and the $TiO_{x<1}$ powder with 16.3 wt.% oxygen could be transformed into pure titanium powder with 0.121 wt.% oxygen by electrodeoxidation at a constant potential of −3.3 V for 10 h. The electrodeoxidation of $TiO_{x<1}$ powder in $CaCl_2$ molten salt follows the step-by-step deoxidation mode, and the lattice of $TiO_{x<1}$ powder after electrodeoxidation shrinks.

Key words: titanium metallurgy; self-propagating high temperature synthesis; titanium powder; electrochemical deoxidation

1 Introduction

Titanium, as a “new metal” produced 80 years ago, is widely used in aerospace, chemical engineering, national defense, military industry, and other technological fields due to its excellent physical and chemical properties [1−4]. Although the application of titanium has been extended to the civil field recently, titanium and titanium alloy components are still expensive compared with steel, aluminum alloy and other engineering parts. The two main reasons could be responsible for the high price of titanium and titanium alloy devices: (1) the commercial extraction technology of titanium, i.e., the Kroll process with intensive energy and capital, has a high cost of titanium extraction [5]; (2) titanium sponge extracted by the Kroll process needs smelting, forging, machining and other processes to prepare the corresponding titanium and titanium alloy devices. Herein, the high reactivity, poor cutting, and machining performance of titanium cause the low utilization rate of raw Ti materials and further increase the cost of titanium components [6,7]. The near-net-shape manufacturing technology of titanium could greatly improve the utilization rate of feedstocks in fabricating Ti components and has the potential to further reduce the price of titanium products. Therefore, improving the extraction technology and near-net-shape manufacturing method of titanium would be an effective path for realizing the low cost of Ti, and some exciting low-cost extraction technologies of titanium powder suitable for near-net-shape

Corresponding author: Zhi-he DOU, Tel/Fax: +86-24-83587260, E-mail: douzh@smm.neu.edu.cn;
Ting-an ZHANG, Tel/Fax: +86-24-83686283, E-mail: zta2000@163.net
DOI: 10.1016/S1003-6326(22)66033-3

manufacturing have been reported, such as Hunter [8], Armstrong [9], TIRO [10], CSIR [11], PRP [12], MER [13], HAMR [14,15], FFC [16,17], OS [18], USTB [19], DDR [20], and two-stage aluminothermic reduction [21]. In addition, some metallurgical approaches for obtaining titanium from Ti-bearing slag also provide novel insight for the low-cost extraction of Ti [22,23]. These developing or developed methods make great contributions to the progress of titanium extraction technology. However, several challenges have been pended to address before the practical industry applications of preparing Ti powder by titanium dioxide [24].

The self-propagating high-temperature synthesis method is a very attractive extraction technique for Ti powder due to its short process, system simplicity, and low cost. Since 1980, the preparation of titanium powder by combustion synthesis has been proposed [25]. Moreover, the uniform Ti powder with 0.2−0.3 wt% oxygen has been generated by combustion synthesis and the deoxidation using calcium [23,26,27]. Although metal calcium has recently been applied as an effective remover for solid oxygen in titanium, it is undeniable that high-priced metal calcium is incapable of decreasing the production cost of titanium powder. And the calcium oxide formed at the interface of titanium powder in the deoxidation process often shows a negative effect on the continuous removal of dissolved oxygen from titanium [28], which results in the difficulty in preparing titanium powder with an oxygen content less than 0.2 wt.%. Fortunately, electrochemical deoxidation, an effective technology removing gas elements in metals [29], has shown great effectiveness in generating low-oxygen Ti lines or recycling Ti sheets due to the low activity of CaO in electrolyte at electrochemical energy [30−32]. Given these technical characteristics including the reaction rapidity of combustion synthesis and the low deoxidation limit of electrodeoxidation in obtaining low-oxygen titanium, in this work, we try combining self-propagating high temperature synthesis with electrodeoxidation (SHS-ED) to fabricate low-oxygen titanium powder and describe the process as two key experimental steps: (1) rapid preparation of nonstoichiometric $TiO_{x<1}$ powder by reducing TiO_2 in combustion mode; (2) electrode-oxidizing $TiO_{x<1}$ to generate low-oxygen titanium powder in $CaCl_2$ molten salt. Details about the preparation of $TiO_{x<1}$ powder by the self-propagating high temperature synthesis of Mg and TiO_2 have been reported in our previous work [20]. The purpose of this work was to describe the concept and process design of SHS-ED process in preparing low-oxygen Ti powder and report the experimental data of key intermediate steps. The obtained results proved that titanium powder with 0.121 wt% oxygen could be successfully prepared from TiO_2 through the SHS-ED process.

2 Experimental

2.1 Preparation of $TiO_{x<1}$ powder

The flow diagram and digital pictures of the corresponding samples for preparing low-oxygen Ti powder by combining SHS and the electrode-oxidation process are shown in Fig. 1, and the experimental details can be found in the following.

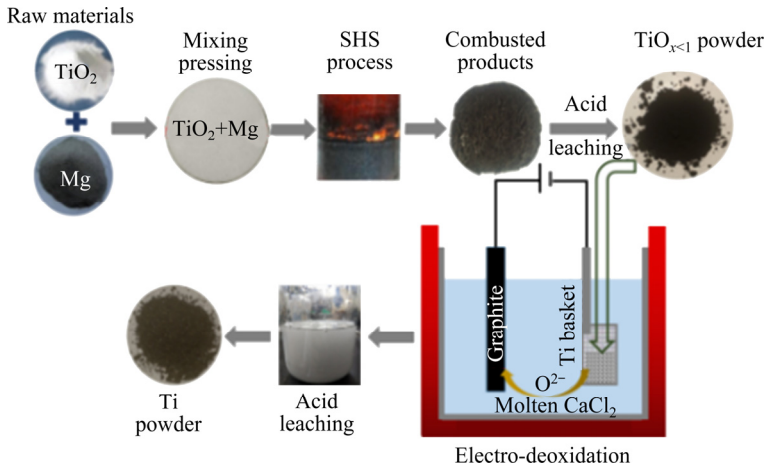

Fig. 1 Flow-sheet and digital pictures of low-oxygen Ti powder fabricated by combining combustion synthesis with electrodeoxidation process

$TiO_{x<1}$ powder was prepared by using rutile TiO_2 (analytical purity >98.5%, ~300 nm) and magnesium powder (analytical purity >99%, 40 μm) as raw materials through SHS. In SHS process, dried TiO_2 and magnesium powder with a molar ratio of 1:2 were mixed and compacted at 10 MPa to generate a mixture block (26 g, 5 cm in diameter, 3 cm in height). And the SHS process was carried out by point heating at the top of the mixture. Then, the SHS products consisting of $TiO_{x<1}$ and MgO phases in our experimental conditions were set in 3% hydrochloric acid (HCl) to eliminate MgO at ambient temperature for 1 h. The impurity ions in acid-leached samples were removed by continuous washing using distilled water, and then the remaining powder was dried in vacuum at 30 °C to obtain $TiO_{x<1}$ powder.

2.2 Electrodeoxidation of $TiO_{x<1}$

Anhydrous $CaCl_2$ (analytical purity ≥96%) as the electrolyte for electrochemical deoxidation was dried in vacuum at 200 °C for more than 48 h, contained in a titanium crucible (purity ≥99.9%, 12 cm in diameter, 15 cm in height) and placed into a gas-tight furnace. The heating process was constructed at 0.01 Pa (setting temperature 900 °C, heating rate 10 °C/min), and high purity argon (analytical purity ≥99.99%, flow rate 0.2 L/min) was introduced into the furnace when the temperature reached the setting temperature. Next, the pre- electrolysis of molten $CaCl_2$ was carried out at 2.8 V for 2 h by utilizing a titanium crucible as the cathode and a high purity graphite rod (diameter 1.2 cm, height 10 cm) as the anode. After pre-electrolysis, the cathode basket (titanium mesh basket, purity ≥99.9%, 100 μm, 1.5 cm in diameter, 3 cm in height) containing $TiO_{x<1}$ (3 g) powder was inserted into the molten $CaCl_2$, and the electrode-oxidation of $TiO_{x<1}$ powder could be conducted. After electrodeoxidation, the cathode basket was lifted to the top of the furnace and cooled in an argon atmosphere. When the temperature in the furnace was low to room temperature, the cathode basket was removed from the furnace and cleaned in distilled water, followed by 3% HCl, distilled water, and alcohol. Then, the filtered samples were dried in vacuum to generate low-oxygen Ti powder.

2.3 Testing and characterization

An electrochemical workstation (Zahner, software Thalex-xt5.6) was used for cyclic voltammetry and current-time tests of $TiO_{x<1}$, where Ti basket with or without $TiO_{x<1}$ was the working electrode, a high-purity graphite anode was the counter electrode, and molybdenum wire (purity ≥99.9%, 0.5 cm in diameter, 10 cm in height) was the reference electrode. X-ray diffractometer with Cu K_α radiation (λ=0.15405 nm, working voltage 40 kV, working current 40 A, step size 0.013°, scanning range (2θ) 20° to 80°) was used to analyze the phase structure. The surface morphology and element composition of the samples were determined by field-emission scanning electron microscopy (Zeiss-Gemini300) and mounted energy dispersive spectrometry (Smart EDX). The particle size distribution and oxygen content of the products were characterized by a laser particle size analyser (Mastersize 3000) and O/N/H analyser (LECO TCH600).

3 Results and discussion

3.1 Preparation of $TiO_{x<1}$ powder by SHS process

Figure 2 shows the XRD patterns of the specimens obtained by self-propagating high temperature synthesis process. The main phases in the SHS products were magnesium oxide, titanium suboxide ($TiO_{0.325}$) and a small amount of TiO ($TiO_{0.97}$). The diffraction peak of MgO could be not found after acid leaching SHS products, and the sample only contained diffraction peaks of $TiO_{0.325}$ and $TiO_{0.97}$, as shown in the inset of Fig. 2.

Figure 3 shows the SEM images and EDS results of SHS products and $TiO_{x<1}$ powder. It can be seen that the SHS products were polygonal

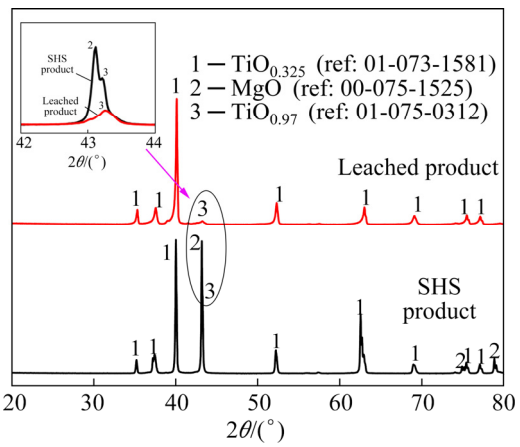

Fig. 2 XRD patterns of SHS samples and corresponding leached products

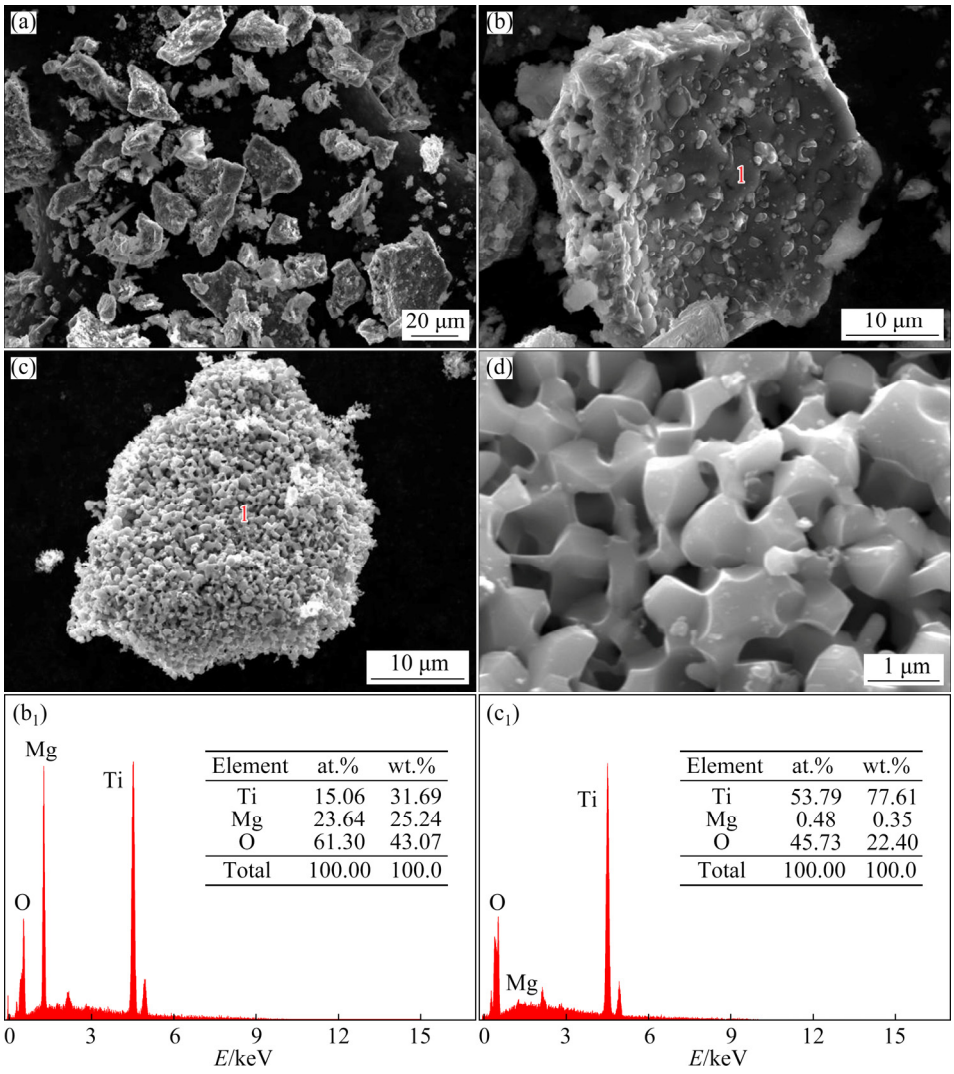

Fig. 3 SEM images (a−d) and EDS results (b_1, c_1) of samples: (a) As-combusted products; (b) Higher magnification of (a); (c) As-combusted products after leaching; (d) Higher magnification of (c); (b_1) EDS results of (b); (c_1) EDS results of (c)

aggregates consisting of numerous particles. The $TiO_{x<1}$ powder had a porous microstructure with an irregular pore size ranging from 100 to 400 nm. It could be speculated that the pore structure of $TiO_{x<1}$ was because of the leaching out of MgO from combusted products according to Figs. 3(b_1) and (c_1). Furthermore, the O/Ti molar ratio of $TiO_{x<1}$ powder was 0.89, it was consistent with XRD results in Fig. 2. The oxygen content of $TiO_{x<1}$ powder was determined to be 16.3 wt.% by O/N/H analysis.

3.2 Electrodeoxidation of $TiO_{x<1}$ powder

To study the electrochemical deoxidation behavior of $TiO_{x<1}$ powder, cyclic voltammetry was carried out in molten $CaCl_2$ with a three-electrode system, where the initial potential was −0.8 V, the minimum potential was −3.3 V, the maximum potential was −0.5 V, and the scanning rate was −30 mV/s. Figure 4 shows the cyclic voltammetry of $TiO_{x<1}$ powder and the blank test measured by the cathode basket without $TiO_{x<1}$ powder, and the relationship between the current peak and the electrochemical reaction is shown in Table 1. It is acceptable that the possible moister or impurities in the easily deliquescent $CaCl_2$ molten salt usually react at the positive potential, while calcium reacts at the more negative potential. However, only a pair of redox peaks (A1, C3) related to calcium deposition and stripping were observed in the blank testing, especially in the negative potential scanning process, which indicated that the pre-electrolysis

process was effective [33,34]. For the $TiO_{x<1}$ powder, when the scanning potential was from −1.2 to −1.4 V, a slight but obvious cathodic current peak C1 was observed, and C1 might be the oxygen removal peak of $TiO_{0.97}$(TiO) according to the XRD results of $TiO_{x<1}$ powder and the thermodynamic reduction potential of TiO at 900 °C [35]. The reduction peak C2 from −1.6 to −1.8 V was considered to be the oxygen ionization peak of dissolved oxygen in $TiO_{0.325}$ powder under electrochemical energy. The current increased linearly when the potential continued to scan negatively until −3.0 V, indicating that the electrochemical reaction was not controlled by diffusion from −1.8 to −3.0 V. Afterward, a downwards current loop was observed at the potential ranging from −3.0 to −2.6 V, which could be attributed to the deposition or nucleation of metal ions on the heterogeneous matrix in electrolyte [34]. When the potential was from −1.4 to −0.7 V, a wide anodic current peak (A1) due to the stripping behavior of calcium deposited on the cathode surface could be observed [36].

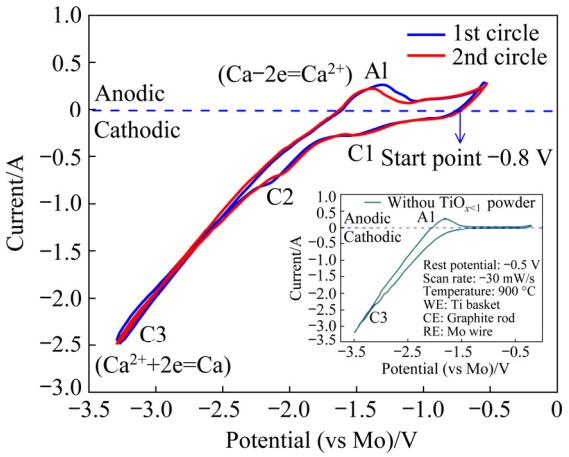

Fig. 4 Cyclic voltammograms in molten $CaCl_2$ with or without $TiO_{x<1}$ powder

Table 1 Relationship between potential corresponding to current peaks and possible electrochemical reactions

Current peak	Scan rate/ ($mV \cdot s^{-1}$)	Potential range (vs Mo)/V	Electrochemical reaction
C1	−30	−1.2 to −1.4	$TiO \rightarrow Ti(O)+O^{2-}$
C2	−30	−1.6 to −1.8	$Ti(O) \rightarrow Ti+O^{2-}$
C3	−30	−2.6 to −3.0	$Ca^{2+} \rightarrow Ca$
A1	30	−1.4 to −0.7	$Ca \rightarrow Ca^{2+}$

Figure 5 shows the current−time curves of electrochemical deoxidizing $TiO_{x<1}$ powder in $CaCl_2$ electrolyte at −3.3 V for 10 h. The background current of the electrodeoxidation process was measured by a cathodic titanium basket without $TiO_{x<1}$ powder, which was about −0.8 A at −3.3 V. From Fig. 5(a), for the electrodeoxidation of $TiO_{x<1}$ powder in $CaCl_2$, the current rapidly decreased from −1.7 to −1.0 A within the initial 1500 s and remained stable for about 700 s, and the current again decreased to −0.8 A after 2200 s until the end of the whole electrodeoxidation process, hence two clear current platforms could be observed in the *I*−*t* curve. These current platforms could be understood by the stepwise electrode-oxidation process of $TiO_{x<1}$ powder in molten salt, i.e., the deoxidation/reduction of $TiO_{0.97}$ occurred first and the corresponding reduction current was high due to its unique defect structure and high oxygen ion mobility [34,37], but the low content of

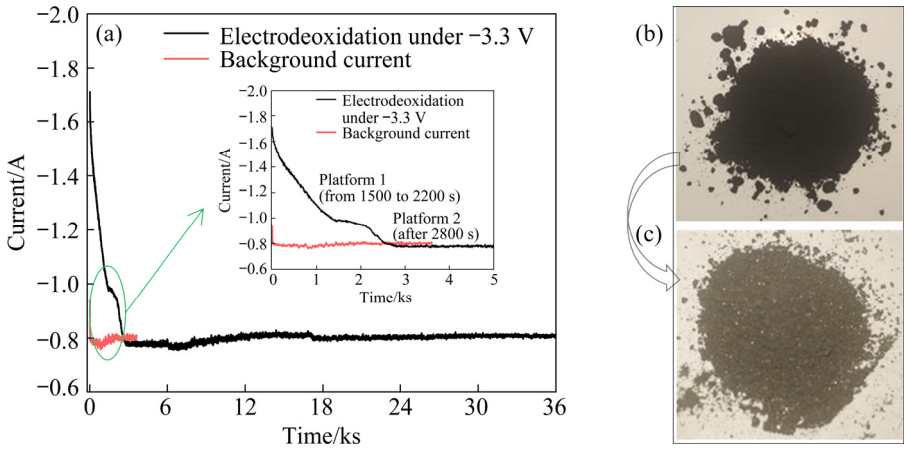

Fig. 5 Electrochemical testing and corresponding photos of products: (a) Current−time plot of $TiO_{x<1}$ measured at −3.3 V for 10 h in two-electrode setup; (b) Digital photo of $TiO_{x<1}$ powder; (c) Digital photo of electrodeoxidized $TiO_{x<1}$ powder

$TiO_{0.97}$ in $TiO_{x<1}$ powder (calculated from the XRD patterns in Fig. 2) resulted in the short lasting time of high current density, shown as Platform 1. Then, the removal of internal oxygen in $TiO_{0.325}$ powder at the electrochemical energy lasted for about 9 h, shown as Platform 2. Digital photos of $TiO_{x<1}$ powder before and after electrodeoxidation are shown in Fig. 5(b), the color change of powder from black to light gray demonstrated that the oxygen content of $TiO_{x<1}$ powder decreased after electrodeoxidation [38].

3.3 Microstructure of electrodeoxidized $TiO_{x<1}$ powder

The XRD patterns of the $TiO_{x<1}$ powder after electrodeoxidation for different durations are shown in Fig. 6. The diffraction peaks related to $TiO_{0.97}$ could not be found in the electrodeoxidized $TiO_{x<1}$ powder for 1 h, which supported the discussion that $TiO_{0.97}$ was first reduced in Fig. 5. The diffraction peak of the electrodeoxidized $TiO_{x<1}$ powder for 10 h was shifted approximately 1° to right compared to the electrodeoxidized $TiO_{x<1}$ powder for 1 h. Moreover, as shown in Table 2, the lattice shrinkage of the $TiO_{x<1}$ powder after electrodeoxidation was obvious, and the lattice parameter c decreased from 4.7751 Å to 4.6860 Å. For the $TiO_{x<1}$ powder, as an ordered or disordered titanium−oxygen solid solution, lattice spacing and lattice parameters would change while the interstitial atoms in the HCP structure were embedded or removed. The lattice contraction was related to the decrease of oxygen content in titanium according to the literature [39,40]. Therefore, the small lattice spacing and lattice parameters of electrodeoxidized Ti powder could be attributed to its fewer interstitial oxygen atoms in crystal. And the analysis result of oxygen content (0.121 wt.%, obtained from the O/N/H analyzer) in the electrodeoxidized Ti powder supported the above consideration.

Figure 7 shows the SEM images and EDS results of electrodeoxidized $TiO_{x<1}$ powder. The electrodeoxidized titanium powder was composed of many agglomerated particles, and the clear sintering necks between particles could be found clearly. And the possible impurity elements, such as magnesium, calcium and chlorine, were not determined in the electrodeoxidized $TiO_{x<1}$ powder as shown in Figs. 7(c, b_1, b_2). The cross section of the electrodeoxidized $TiO_{x<1}$ powder can be seen in Fig. 7(d), the pore structure in three dimensions

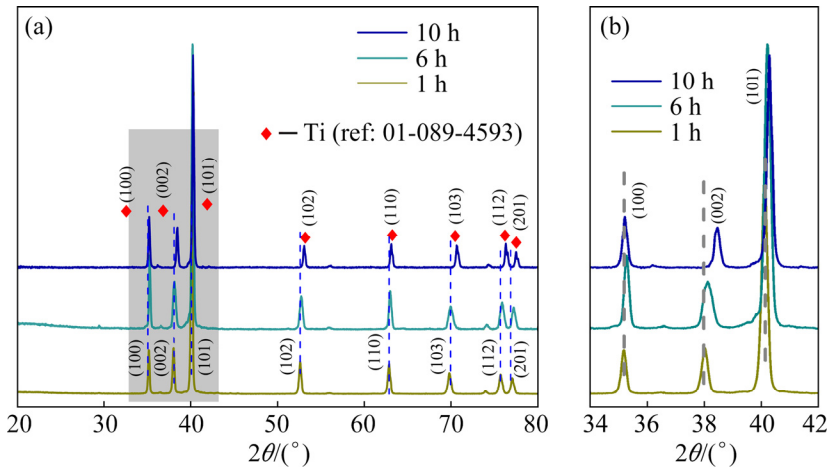

Fig. 6 XRD patterns of $TiO_{x<1}$ powder after electrodeoxidation for 1, 6, and 10 h (a), and enlarged patterns (b) of (a) from 34° to 42°

Table 2 d-space and lattice parameters of $TiO_{x<1}$ powder before and after electro-deoxidation for 10 h (Wavelength = 1.54 Å (Cu K_α))

Sample	d-space/Å			a/Å	c/Å
	(100)	(002)	(101)		
$TiO_{x<1}$ powder	2.5721	2.3875	2.2644	2.9700	4.7751
Ti powder after deoxidation for 10 h	2.5547	2.3430	2.2430	2.9500	4.6860

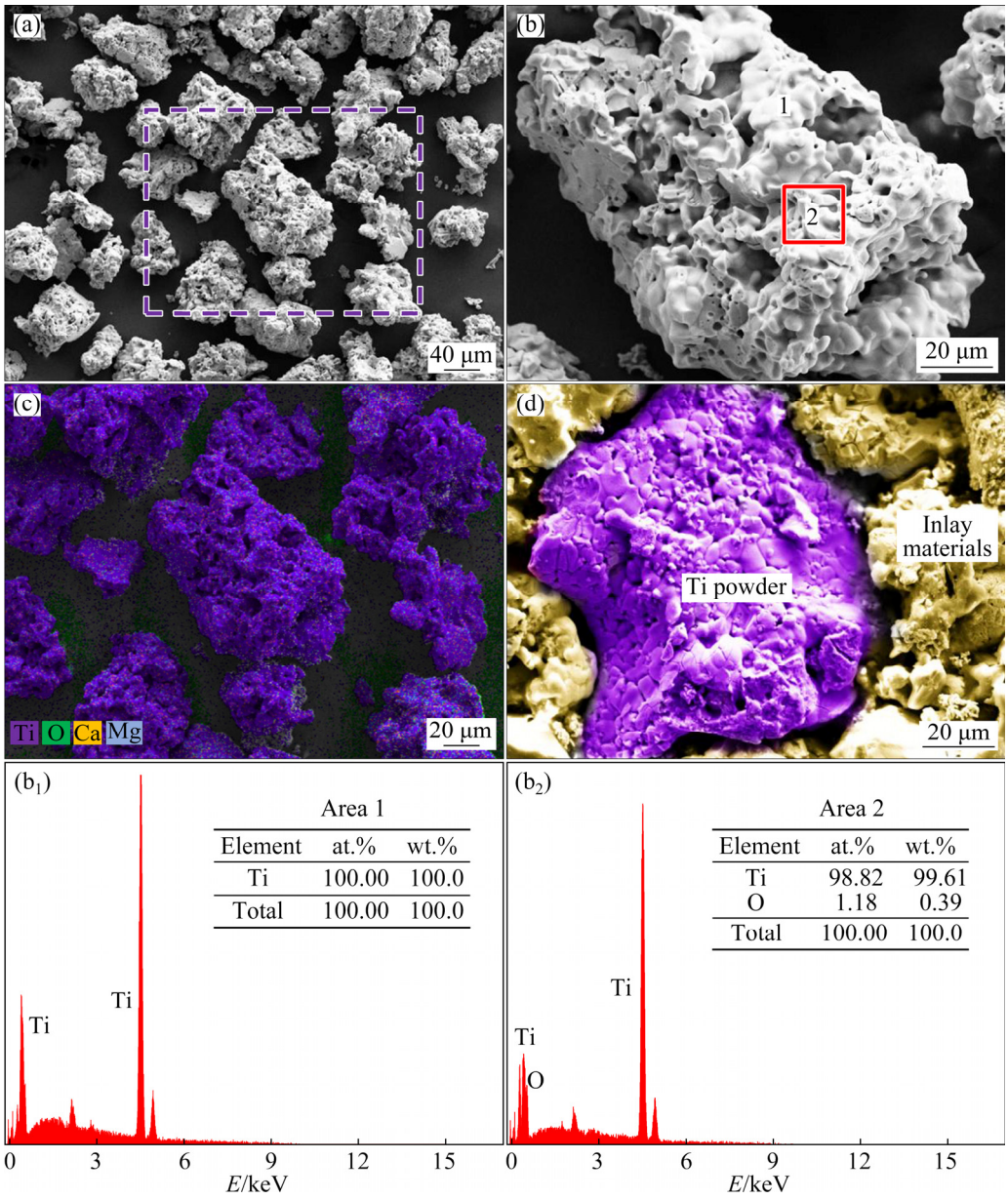

Fig. 7 SEM images (a−d) and EDS results (b_1, b_2) of samples: (a) Electrodeoxidized Ti powder for 10 h; (b) Higher magnification of (a); (c) EDS mapping of labeled part in (a); (d) Cross-section of electrodeoxidized Ti powders; (b_1, b_2) EDS results of (b)

of electrodeoxidized $TiO_{x<1}$ powder made it possible to be used as potential feeds in preparing bone implants. A guess could be made according to the oxygen content and morphology change of electrodeoxidized $TiO_{x<1}$ powder, i.e., the oxygen removing and the sintering/growth of titanium particles were concurrent in the electrodeoxidation of $TiO_{x<1}$ powder. Consequently, as shown in Fig. 8, the particle size of $TiO_{x<1}$ powder after electrodeoxidation for 10 h increased from 25.78 to 79.91 μm.

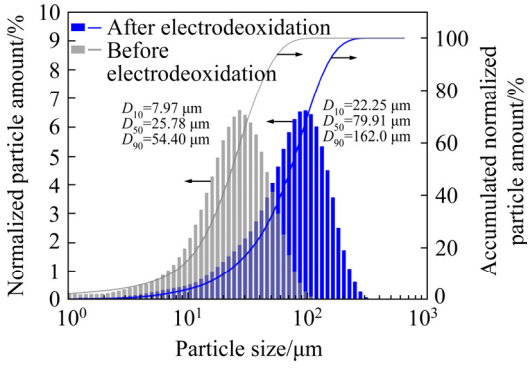

Fig. 8 Particle distribution of $TiO_{x<1}$ powder before and after electrodeoxidation

4 Conclusions

(1) A mixture of $TiO_{0.325}$ and $TiO_{0.97}$ was synthesized after acid leaching MgO in the SHS products prepared with TiO_2 to Mg molar ratio of 1:2.

(2) The deoxidation of the $TiO_{x<1}$ powder was conducted step by step from the cyclic voltammetry and current−time results, and the oxygen content of $TiO_{x<1}$ powder after electrodeoxidation for 10 h was decreased from 16.3 to 0.121 wt.%.

(3) The *d*-space and lattice parameters of electrodeoxidized $TiO_{x<1}$ powder were less than those of the $TiO_{x<1}$ powder. The particle size of $TiO_{x<1}$ powder after electrodeoxidation for 10 h was 79.91 μm.

(4) Low-oxygen Ti powder was successfully synthesized from TiO_2 by the SHS-ED process. This is the first attempt to fabricate low-oxygen Ti powder by SHS-ED, and the satisfactory results indicate the potential availability of electrode-oxidation technology in oxygen removal of active metal powder.

Acknowledgments

This work was financially supported by the National Natural Science Foundation of China (Nos. 52174333, U1908225, 1702253), and the Fundamental Research Funds for Central Universities, China (Nos. N182515007, N170908001, N2025004).

References

[1] FANG Z Z, PARAMORE J D, SUN P, CHANDRAN K S R, ZHANG Y, XIA Y, CAO F, KOOPMAN M, FREE M. Powder metallurgy of titanium – Past, present, and future [J]. International Materials Reviews, 2018, 63: 407−459.

[2] MA Q. Cold compaction and sintering of titanium and its alloys for near-net-shape or preform fabrication [J]. International Journal of Powder Metallurgy, 2010, 46: 29−44.

[3] PENG He-li, LI Xi-feng, CHEN Xu, JIANG Jun, LUO Jing-feng, XIONG Wei, CHEN Jun. Effect of grain size on high-temperature stress relaxation behavior of fine-grained TC4 titanium alloy [J]. Transactions of Nonferrous Metals Society of China, 2020, 30: 668−677.

[4] WANG Zhen-yu, LIU Li-bin, WU Di, ZHANG Li-gang, WANG Wan-li, ZHOU Ke-chao. α'' phase-assisted nucleation to obtain ultrafine α precipitates for designing high-strength near-β titanium alloys [J]. Transactions of Nonferrous Metals Society of China, 2020, 30: 2681−2696.

[5] TAKEDA O, OUCHI T, OKABE T H. Recent progress in titanium extraction and recycling [J]. Metallurgical and Materials Transactions B, 2020, 51: 1315−1328.

[6] ZHU Xiao-fang, LI Qing, ZHANG Ying, FANG Zhi-gang, ZHENG Shi-li, SUN Pei, XIA Yang. Mini-review on the preparation of titanium metal by the thermochemical processes [J]. The Chinese Journal of Process Engineering, 2019, 19: 456−464. (in Chinese)

[7] ZHANG Y, LU W L, SUN P, FANG Z Z, QIAO S, ZHANG Y, ZHENG S L. Deoxygenation of Ti metal: A review of processes in literature [J]. International Journal of Refractory Metals and Hard Materials, 2020, 91: 105270.

[8] HUNTER M A. Metallic titanium [J]. Journal of the American Chemical Society, 1910, 32: 330−336.

[9] CROWLEY G. How to extract low-cost titanium [J]. Advanced Materials and Processes, 2003, 161: 25−27.

[10] DOBLIN C, FREEMAN D, RICHARDS M. The TiRO™ process for the continuous direct production of titanium powder [J]. Key Engineering Materials, 2013, 551: 37−43.

[11] VUUREN D S, OOSTHUIZEN S, HEYDENRYCH M. Titanium production via metallothermic reduction of $TiCl_4$ in molten salt: Problems and products [J]. Journal of the Southern African Institute of Mining and Metallurgy, 2011, 111: 1−31.

[12] OKABE T H, ODA T, MITSUDA Y. Titanium powder production by preform reduction process (PRP) [J]. Journal of Alloys and Compounds, 2004, 364: 156−163.

[13] PARK I, ABIKO T, OKABE T H. Production of titanium powder directly from TiO_2 in $CaCl_2$ through an electronically mediated reaction (EMR) [J]. Journal of Physics and Chemistry of Solids, 2005, 66: 410−413.

[14] ZHANG Y, FANG Z Z, SUN P, ZHANG T Y, XIA Y, ZHOU C S, HUANG Z. Thermodynamic destabilization of Ti−O solid solution by H_2 and deoxygenation of Ti using Mg [J]. Journal of the American Chemical Society, 2016, 138: 6916−6919.

[15] XIA Y, FANG Z Z, ZHANG Y, LEFLER H, ZHANG T Y, SUN P, HUANG Z. Hydrogen assisted magnesiothermic reduction (HAMR) of commercial TiO_2 to produce titanium powder with controlled morphology and particle size [J]. Materials Transactions, 2016, 58: 355−360.

[16] CHEN G Z, FRAY D J, FARTHING T W. Direct electrochemical reduction of titanium dioxide to titanium in molten calcium chloride [J]. Nature, 2000, 407: 361−364.

[17] CHEN G Z. Interactions of molten salts with cathode products in the FFC Cambridge Process [J]. International Journal of Minerals, Metallurgy and Materials, 2020, 27: 1572−1587.

[18] SUZUKI R O, INOUE S. Calciothermic reduction of titanium oxide in molten $CaCl_2$ [J]. Metallurgical and Materials Transactions B, 2003, 34: 277−285.

[19] WANG Q Y, SONG J X, WU J Y, JIAO S Q, HOU J G, ZHU H M. A new consumable anode material of titanium oxycarbonitride for the USTB titanium process [J]. Physical Chemistry Chemical Physics, 2014, 16: 8086−8091.

[20] FAN S G, DOU Z H, ZHANG T A, LIU Y, NIU L P. Deoxidation mechanism in reduced titanium powder prepared by multistage deep reduction of TiO_2 [J]. Metallurgical and Materials Transactions B, 2019, 50: 282−290.

[21] ZHAO K, FENG N X, WANG Y W. Fabrication of Ti-Al intermetallics by a two-stage aluminothermic reduction process using Na_2TiF_6 [J]. Intermetallics, 2017, 85: 156−162.
[22] FAN G Q, WANG M, DANG J, ZHANG R, LV Z P, HE W C, LV X W. A novel recycling approach for efficient extraction of titanium from high-titanium-bearing blast furnace slag [J]. Waste Management, 2021, 120: 626−634.
[23] PU Z H, JIAO H D, MI Z S, WANG M Y, JIAO S Q. Selective extraction of titanium from Ti-bearing slag via the enhanced depolarization effect of liquid copper cathode [J]. Journal of Energy Chemistry, 2020, 42:43−48.
[24] ZHANG Y, FANG Z Z, SUN P, ZHENG S L, XIA Y, FREE M. A perspective on thermochemical and electrochemical processes for titanium metal production [J]. JOM, 2017, 69: 1861−1868.
[25] FROLOV J V, FETZOY V P. Synthesis of submicron titanium powder under the combustion mode [C]//The First All-Union Symposium on Macroscopic Kinetics and Chemical Gasodynamics. Chernogolovka , 1984: 13−14.
[26] NERSISYAN H H, WON H I, WON C W, JO A, KIM J H. Direct magnesiothermic reduction of titanium dioxide to titanium powder through combustion synthesis [J]. Chemical Engineering Journal, 2014, 235: 67−74.
[27] WON C W, NERSISYAN H H, WON H I. Titanium powder prepared by a rapid exothermic reaction [J]. Chemical Engineering Journal, 2010, 157: 270−275.
[28] SUZUKI R O, ONO K, TERANUMA K. Calciothermic reduction of titanium oxide and in-situ electrolysis in molten $CaCl_2$ [J]. Metallurgical and Materials Transactions B, 2003, 34: 287−295.
[29] WARD R G, HOAR T P. The electrolytic removal of oxygen, sulphur, selenium, and tellurium from molten copper [J]. Institute of Metals, 1962, 90: 6−12.
[30] OKABE T H, NAKAMURA M, OISHI T, ONO K. Electrochemical deoxidation of titanium [J]. Metallurgical and Materials Transactions B, 1993, 24: 449−455.
[31] TANINOUCHI Y K, HAMANAKA Y, OKABE T H. Electrochemical deoxidation of titanium and its alloy using molten magnesium chloride [J]. Metallurgical and Materials Transactions B, 2016, 47: 3394−3404.
[32] OKABE T H, HAMANAKA Y, TANINOUCHI Y K. Direct oxygen removal technique for recycling titanium using molten $MgCl_2$ salt [J]. Faraday Discussions, 2016, 190:109−126.
[33] CHEN G, FRAY D. Voltammetric studies of the oxygen-titanium binary system in molten calcium chloride [J]. Journal of the Electrochemical Society, 2002, 149: E455−E467.
[34] DRING K, DASHWOOD R, INMAN D. Voltammetry of titanium dioxide in molten calcium chloride at 900 °C [J]. Journal of the Electrochemical Society, 2005, 152: E104−E113.
[35] BARIN I, PLATZKI G. Thermochemical data of pure substances [M]. 3rd ed. Weinheim: VCH, 1997.
[36] CHEN G, KINLOCH I, SHAFFER M S P, FRAY D, WINDLE A. Electrochemical investigation of the formation of carbon nanotubes in molten salts [J]. High Temperature Material Processes, 1998, 2: 459−469.
[37] VALEEVA A A, TANG G, GUSEV A I, REMPEL' A A. Observation of structural vacancies in titanium monoxide using transmission electron microscopy [J]. Physics of the Solid State, 2003, 45: 87−93.
[38] XIA Y, ZHAO J L, TIAN Q H, GUO X Y. Review of the effect of oxygen on titanium and deoxygenation technologies for recycling of titanium metal [J]. JOM, 2019, 71: 3209−3220.
[39] XIA Y, FANG Z Z, FAN D Q, SUN P, ZHANG Y, ZHU J. Hydrogen enhanced thermodynamic properties and kinetics of calciothermic deoxygenation of titanium-oxygen solid solutions [J]. International Journal of Hydrogen Energy, 2018, 43: 11939−11951.
[40] KIM H L, YUN C G, JU J H, JUN H J, LEE H J, HA H. Deoxidation behavior of Zr powder manufactured by using self-propagating high-temperature synthesis with Mg reducing agent [J]. Metallurgical and Materials Transactions B, 2020, 51: 1070−1078.

自蔓延高温合成−电化学脱氧制备低氧钛粉

周新宇[1,2]，豆志河[1,2]，张廷安[1,2]，闫基森[2]，闫建鹏[2]

1. 东北大学 多金属共生矿生态冶金教育部重点实验室，沈阳 110819；
2.东北大学 冶金学院，沈阳 110819

摘　要：报道一种自蔓延高温合成−电化学脱氧制备低氧钛粉的新工艺，该工艺包含两个重要的实验步骤：(1)自蔓延模式下镁热还原 TiO_2 快速制备非化学计量比的低价钛氧化物 $TiO_{x<1}$ 粉末(高氧含量钛粉)；(2)$CaCl_2$ 熔盐体系中 $TiO_{x<1}$ 粉末的电化学脱氧。通过 XRD、SEM 等物相分析、微观结构表征手段和电化学测试技术分析关键中间步骤的实验结果。结果表明：TiO_2:Mg 摩尔比为 1:2 的自蔓延高温合成产物酸洗后可得到 $TiO_{x<1}$ 粉末($TiO_{0.325}$ 和 $TiO_{0.97}$)，在 $CaCl_2$ 熔盐中施加−3.3 V 恒电位电化学脱氧 10 h 可将含 16.3%氧(质量分数)的 $TiO_{x<1}$ 粉末转化为氧含量低至 0.121%(质量分数)的低氧钛粉，$TiO_{x<1}$ 粉体在 $CaCl_2$ 熔盐中的电化学脱氧遵循分步脱氧模式，脱氧后钛粉晶格明显收缩。

关键词：钛冶金；自蔓延高温合成；钛粉；电化学脱氧

(Edited by Xiang-qun LI)